Transition-State Analysis

Origin of Diastereoselection in the Hydrosilylation of Chiral *N*-Acyliminium Intermediates Derived from Pyroglutamic Acid

Makoto Oba, Shinichi Koguchi, Kozaburo Nishiyama,* Daisuke Kaneno, and Shuji Tomoda**

The reaction of *N*-acyliminium intermediates with various nucleophiles has been widely used as a key step in the synthesis of many nitrogen-containing compounds.[1] In particular, optically active *N*-acyliminium ions derived from L-pyroglutamic acid are versatile intermediates in the synthesis of naturally occurring compounds and chiral auxiliaries.[2] Generally, the nucleophilic attack of silicon reagents such as cyanosilane and allylsilane to these intermediates derived from pyroglutaminol has been reported to give predominantly *anti* adducts.[3,4] In contrast, the *N*-acyliminium ions prepared from pyroglutamate derivatives undergo *syn*-selective addition of silicon nucleophiles.[3,5] Namely, the stereochemistry of the nucleophilic attack can be controlled depending on whether the side chain of the iminium intermediate is an ester or a reduced form such as a hydroxymethyl group.

Recently, we reported the stereodivergent synthesis of two isotopomeric [3,4,5-D_3]prolines for NMR structure determination of polypeptides.[6] The stereochemistry of the deuterium substitution at the 5-position of the proline ring can be controlled by taking advantage of the previously mentioned substituent dependency. Although the *anti* preference observed in the nucleophilic attack on the iminium intermediates derived from pyroglutaminol is attributable to the steric interaction between the nucleophile and the hydroxymethyl group of the intermediates, the origin of the reversed face selectivity found in the reaction of iminium intermediates carrying the ester substituent cannot be fully explained at the present stage.

Table 1 shows selected data for the diastereoselective deuteration of the iminium intermediate derived from hemiaminal **1** leading to the deuterated prolinol or proline derivative **2** (Scheme 1).[6] In the present work, we studied the hydrosilylation of iminium ions by quantum-chemical calculations using model compounds.

Table 1: Diastereoselective deuteration of iminium intermediate derived from **1**.[a]

Entry	R	Deuteride	*syn*:*anti*, **2**
1	CH_2OSiMe_2tBu	Et_3SiD	13:87
2	CH_2OSiMe_2tBu	Ph_3SiD	8:92
3	CH_2OSiMe_2tBu	$(Me_3Si)_3SiD$	3:97
4	CH_2OSiPh_2tBu	$(Me_3Si)_3SiD$	1:99
5	CO_2Et	Et_3SiD	87:13
6	CO_2Et	Ph_2SiD_2	59:41
7	CO_2Et	Ph_3SiD	55:45
8	CO_2Et	$(Me_3Si)_3SiD$	74:26

[a] See ref. [6].

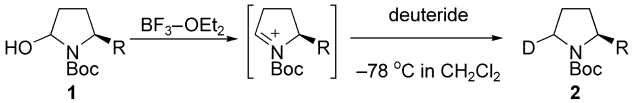

Scheme 1. Diastereoselective deuteration of iminium intermediate derived from **1**.

The geometries of iminium intermediates **I** and **II** derived from pyroglutaminol and pyroglutamate, respectively, were fully optimized and characterized by frequency analysis at the B3LYP/6-31G(d) level (Figure 1).[7] Since the π-facial selection in nucleophilic attack on the cyclic iminium intermediates depends on facial difference in the driving force operating in the exterior region of the substrate, the exterior frontier orbital extension model (EFOE model)[8] was employed to evaluate quantitatively the steric and electronic environment around the π face of the iminium intermediates **I** and **II** (Table 2).

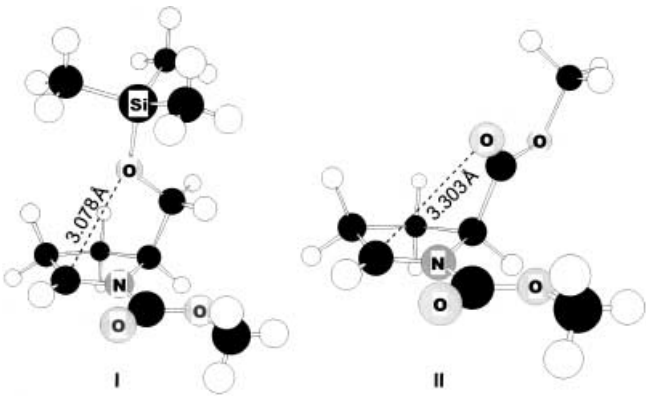

Figure 1. B3LYP/6-31G(d)-optimized structures of intermediates **I** and **II** derived from pyroglutaminol and pyroglutamate, respectively.

As pointed out by Shono et al. and Langlois et al.,[3] an interaction of the cationic iminium carbon with the oxygen atom of the side chain was observed in the intermediate **I** (C–O distance = 3.078 Å).[9] The PDAS value of the *syn* face of **I** (28.6 au^3) is much less than that of the *anti* face (101.7 au^3) owing to the bulky silyl protective group. Since the facial difference in the EFOE densities are not so large, the

[*] Dr. M. Oba, S. Koguchi, Prof. K. Nishiyama
Department of Material Science and Technology
Tokai University
Shizuoka 410-0395 (Japan)
Fax: (+81) 55-968-1155
E-mail: makoto@wing.ncc.u-tokai.ac.jp
nishiyam@wing.ncc.u-tokai.ac.jp
Dr. D. Kaneno, Prof. S. Tomoda
Department of Life Sciences
Graduate School of Arts and Sciences
The University of Tokyo
Tokyo 153-8902 (Japan)
Fax: (+81) 3-5454-6998
E-mail: tomoda@selen.c.u-tokyo.ac.jp

  DOI: 10.1002/ange.200353366

Table 2: EFOE analysis of the iminium intermediates **I** and **II**.[a]

Iminium int.	PDAS [au^3]		EFOE density [%]		
	syn	*anti*	MO	*syn*	*anti*
I	28.6	101.7	LUMO	1.22 ($C_{C=N}$)	1.48 ($C_{C=N}$)
II	57.4	113.0	LUMO	1.55 ($C_{C=N}$)	1.90 ($C_{C=N}$)
			HOMO	1.03 ($O_{C=O}$)	–

[a] See ref. [8] for the conditions of the EFOE analysis. PDAS = π-plane-divided accessible space.

preferential *anti* attack of a nucleophile to the intermediate **I** is explained mainly by the steric congestion on its *syn* face. In fact, the bulkier the silyl protective group and the silicon nucleophile are, the higher the *anti* selectivity becomes (Table 1, entries 1–4).

In the case of the iminium intermediate **II**, the *syn* addition is favored despite unfavorable steric congestion around the *syn* face (PDAS = 57.4 au^3) compared to that of the *anti* face (PDAS = 113.0 au^3). The strong affinity of oxygen to a silicon atom is well known. Attractive interactions such as orbital and electrostatic interactions between the carbonyl oxygen in the side chain of the intermediate **II** and the silicon reagent can provide the driving force for the *syn* attack. The difference between the *syn* and *anti* face of **II** in terms of the EFOE densities of the LUMO at the reaction center is very small, and even slightly favors the *anti* attack; however, the extension of the HOMO, which mainly corresponds to the lone pairs of the ester carbonyl oxygen, is very large (EFOE density = 1.03 %). Natural bond orbital (NBO) analyses[11] of the prereaction complex as well as the transition state (vide infra) for the *syn* attack show the presence of orbital interactions between the oxygen lone pairs and the silicon nucleophile. To minimize unfavorable steric repulsion caused upon *syn* attack, the smaller nucleophile is advantageous (Table 1, entries 5–8).

We also carried out transition-state analysis. The fully B3LYP/6-31G(d,p)-optimized transition structures *anti*-**TS-I** and *syn*-**TS-I** from the reaction of trimethylsilane with iminium intermediate **I** are shown in Figure 2. Analytical harmonic frequencies at the same level were used to characterize the nature of the structures and to evaluate the vibrational energy and the zero-point vibrational energy (ZPVE) correction. Each transition-state structure had a single imaginary vibrational frequency, $\nu_i = -156$ and $-159\ \mathrm{cm}^{-1}$ for *anti*-**TS-I** and *syn*-**TS-I**, respectively, corresponding to the stretching vibration of the forming C–H bond. The *anti*-**TS-I** is $0.979\ \mathrm{kcal\,mol}^{-1}$ [B3LYP/6-311 + G(2d,p)//B3LYP/6-31G(d,p) including ZPVE correction scaled by 0.9804[12]] more stable than the *syn*-**TS-I** in good agreement with the experimental observations (Table 1, entries 1–4).[13] The structure of the iminium fragment in *anti*-**TS-I** is substantially similar to that of ground-state iminium intermediate **I** except for the direction of the siloxymethyl side chain, whereas *syn*-**TS-I** has geometrical distortion in the iminium moiety to minimize steric repulsion between the incoming silane and the side chain. The relative stabilities of the *syn* and *anti* transition states would be mainly determined by geometrical distortion in the iminium moiety caused by nucleophilic attack of the silane.

The transition structures *syn*-**TS-II** ($\nu_i = -535\ \mathrm{cm}^{-1}$) and *anti*-**TS-II** ($\nu_i = -580\ \mathrm{cm}^{-1}$) for the hydrosilylation of iminium intermediate **II** optimized at the HF/6-31G(d,p) level are shown in Figure 3. As predicted by the experimentally observed π-face selectivity (Table 1, entries 5–8), *syn*-**TS-II** is $1.01\ \mathrm{kcal\,mol}^{-1}$ [MP2/6-311 + G(d,p)//HF/6-31G(d,p) including ZPVE correction scaled by 0.9135[14]] lower in energy than *anti*-**TS-II**.[15] Based on AM1 calculations, Lhommet and co-workers proposed that the *syn* attack is preferred owing to a relief in the steric hindrance existing between the two methoxycarbonyl groups.[4d] However, our calculation shows that the dihedral angle between the two methoxycarbonyl groups in *syn*-**TS-II** is 11.3° smaller than that in *anti*-**TS-II**, indicating such steric interaction does not play a role in the diastereoface selection. Why is *syn*-**TS-II** lower in energy than *anti*-**TS-II** despite the presence of unfavorable steric interaction between the approaching silicon nucleophile and the ester side chain? NBO analysis

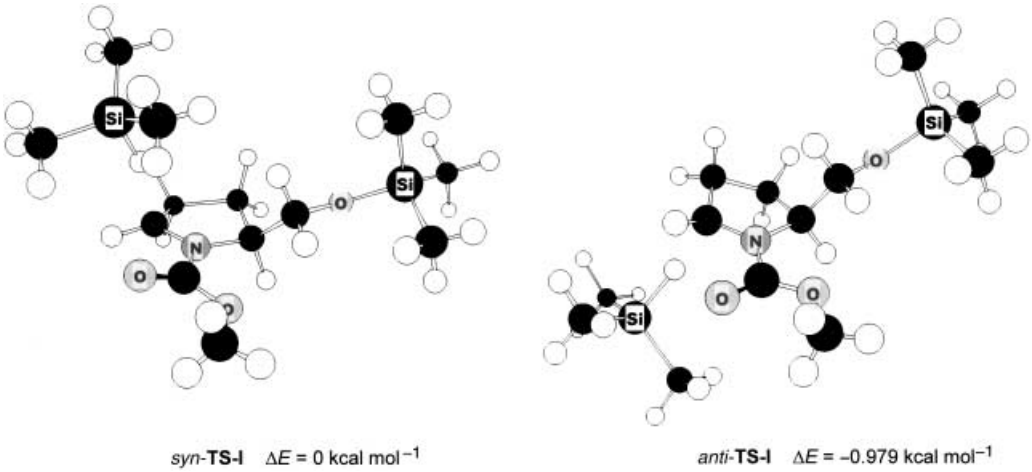

Figure 2. B3LYP/6-31G(d,p)-optimized structures and relative energies [B3LYP/6-311 + G(2d,p)] of transition states for the reaction of trimethylsilane with intermediate **I**.

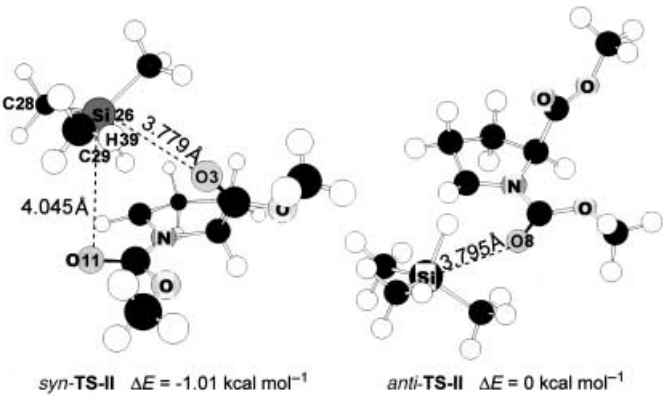

Figure 3. HF/6-31G(d,p)-optimized structures and relative energies [MP2/6-311+G(d,p)] of transition states for the reaction of trimethylsilane with intermediate **II**.

indicates the presence of orbital interactions between the lone pairs of the urethane carbonyl oxygen and antibonding orbitals in the silicon reagent both in *syn*-**TS-II** and in *anti*-**TS-II**. The total amount of the delocalization energies for the lone-pair electrons of O8 in *anti*-**TS-II** (0.75 kcal mol^{-1}) is slightly greater than that for O11 lone pair electrons in *syn*-**TS-II** (0.34 kcal mol^{-1}). However, overwhelmingly stronger orbital interactions (1.76 kcal mol^{-1}) are found between the lone pairs of the ester carbonyl oxygen O3 and the silicon reagent in *syn*-**TS-II**. The most important contributions to the above interactions are two $n_{O3} \rightarrow \sigma^*$ interactions involving Si26–C28 and C29–H39 antibonds as acceptors and their delocalization energies are 0.63 and 0.55 kcal mol^{-1}, respectively, where favorable overlap between the lone pairs of O3 and the backlobe of the antibonding orbitals allows stronger delocalization.[16] Thus, *syn*-**TS-II** benefits from these orbital interactions involving O3 lone pairs as donors, whereas such interactions cannot appear in *anti*-**TS-II**. We can therefore conclude that the attractive interactions between the silicon reagent and the ester side chain are chiefly responsible for stabilizing *syn*-**TS-II**.

In summary, the *anti* selectivity observed in the hydrosilylation of the iminium intermediate **I** derived from pyroglutaminol is rationalized by unfavorable steric effects caused upon *syn* attack both in the ground state and in the transition state. The dramatic reversal of the favored direction of the nucleophilic attack found in the reaction of intermediate **II** bearing the ester substituent is best explained by the attractive interaction between the silicon nucleophile and the ester side chain. The orbital and/or electrostatic interactions involving the ester carbonyl oxygen can have a significant influence on the *syn*-selective hydrosilylation. Experimentally, the choice of a tin nucleophile over silanes and toluene over dichloromethane as a solvent proved to be more efficient for the *syn*-selective hydrometalations.[6] The explanation of the reagent and solvent effects on the *syn* addition awaits theoretical verification. Studies that address these issues are currently in progress.

Received: November 19, 2003 [Z53366]

Keywords: diastereoselectivity · hydrosilylation · iminium intermediates · transition states

[1] W. N. Speckamp, K. J. Moolenaar, *Tetrahedron* **2000**, *56*, 3817.
[2] C. Nájera, M. Yus, *Tetrahedron: Asymmetry* **1999**, *10*, 2245; M. Pichon, B. Figadère, *Tetrahedron: Asymmetry* **1996**, *7*, 927.
[3] N. Langlois, A. Rojas-Rousseau, O. Decavallas, *Tetrahedron: Asymmetry* **1996**, *7*, 1095; N. Langlois, A. Rojas, *Tetrahedron* **1993**, *49*, 77; T. Shono, T. Fujita, Y. Matsumura, *Chem. Lett.* **1991**, 81.
[4] a) J. Åhman, P. Somfai, *Tetrahedron* **1992**, *48*, 9537; b) K.-H. Altmann, *Tetrahedron Lett.* **1993**, *34*, 7721; c) T. Katoh, Y. Nagata, Y. Kobayashi, K. Arai, J. Minami, S. Terashima, *Tetrahedron Lett.* **1993**, *34*, 5743; d) H. Dhimane, C. V. Bacqué, L. Hamon, G. Lhommet, *Eur. J. Org. Chem.* **1998**, 1955.
[5] E. J. Corey, P.-W. Yuen, F. J. Hannon, D. A. Wierda, *J. Org. Chem.* **1990**, *55*, 784; M. Thaning, L.-G. Wistrand, *Acta Chem. Scand.* **1992**, *46*, 194.
[6] M. Oba, A. Miyakawa, K. Nishiyama, T. Terauchi, M. Kainosho, *J. Org. Chem.* **1999**, *64*, 9275; M. Oba, T. Terauchi, J. Hashimoto, T. Tanaka, K. Nishiyama, *Tetrahedron Lett.* **1997**, *38*, 5515.
[7] Gaussian 98 (Revision A.11.4), M. J. Frisch, G. W. Trucks, H. B. Schlegel, G. E. Scuseria, M. A. Robb, J. R. Cheeseman, V. G. Zakrzewski, J. A. Montgomery, R. E. Stratmann, J. C. Burant, S. Dapprich, J. M. Millam, A. D. Daniels, K. N. Kudin, M. C. Strain, O. Farkas, J. Tomasi, V. Barone, M. Cossi, R. Cammi, B. Mennucci, C. Pomelli, C. Adamo, S. Clifford, J. Ochterski, G. A. Petersson, P. Y. Ayala, Q. Cui, K. Morokuma, D. K. Malick, A. D. Rabuck, K. Raghavachari, J. B. Foresman, J. Cioslowski, J. V. Ortiz, B. B. Stefanov, G. Liu, A. Liashenko, P. Piskorz, I. Komaromi, R. Gomperts, R. L. Martin, D. J. Fox, T. Keith, M. A. Al-Laham, C. Y. Peng, A. Nanayakkara, C. Gonzalez, M. Challacombe, P. M. W. Gill, B. G. Johnson, W. Chen, M. W. Wong, J. L. Andres, M. Head-Gordon, E. S. Replogle, J. A. Pople, Gaussian, Inc., Pittsburgh, PA, **1998**.
[8] The EFOE model assumes that FMO extension (exterior frontier orbital electron density = EFOE density for LUMO or HOMO in the present cases) and reagent-accessible space (steric effects; π-plane-divided accessible space = PDAS value) outside the molecular surface (van der Waals surface) of the reactant should be the major factors of facial stereoselection. EFOE analysis was performed at the HF/6-31G(d) level with a lattice mesh of 0.1 au. Molecular surface was defined by Bondi's van der Waals radii. Integration of EFOE density was performed up to 10 au from the van der Waals surface. PDAS integration was performed up to 5 au from the van der Waals surface. S. Tomoda, *Chem. Rev.* **1999**, *99*, 1243; S. Tomoda, J. Zhang, D. Kaneno, M. Segi, A. Zhou, *Tetrahedron Lett.* **2000**, *41*, 4597; S. Tomoda, D. Kaneno, T. Senju, *Heterocycles* **2000**, *52*, 1435; Y. Ikuta, S. Tomoda, *Tetrahedron Lett.* **2003**, *44*, 5931; D. Kaneno, S. Tomoda, *Org. Lett.* **2003**, *5*, 2947.
[9] The energy difference between the collapsed and the corresponding open form of the intermediate **I** at the B3LYP/6-311+G(2d,p) level is 4.07 kcal mol^{-1} in favour of the collapsed form. The inclusion of solvent effects from CH_2Cl_2 using Tomasi's PCM method[10] at the B3LYP/6-311+G(d,p) level does not change the result and also favors the collapsed form by 3.40 kcal mol^{-1}.
[10] S. Miertus, E. Scrocco, J. Tomasi, *Chem. Phys.* **1981**, *55*, 117.
[11] A. E. Reed, L. A. Curtiss, F. Weinhold, *Chem. Rev.* **1988**, *88*, 899.
[12] C. W. Bauschlicher, Jr., H. Partridge, *J. Chem. Phys.* **1995**, *103*, 1788.
[13] The reaction barriers for the *anti* and *syn* attack with respect to the prereaction complexes calculated at the B3LYP/6-311+G(2d,p) level are 2.09 and 2.81 kcal mol^{-1}, respectively. The geometries of the prereaction complexes for the *anti* and *syn*

attack were located by the intrinsic reaction coordinate (IRC) calculations [HF/3-21G(d)] starting from *anti*-**TS-I** and *syn*-**TS-I**, respectively, followed by full optimization at the B3LYP/6-31G(d,p) level.

[14] J. A. Pople, A. P. Scott, M. W. Wong, L. Radom, *Isr. J. Chem.* **1993**, *33*, 345.

[15] In the case of *syn*-**TS-II**, we could not obtain the appropriate structure at the B3LYP/6-31G(d,p) level. Therefore, the relative energies are evaluated using MP2 as well as B3LYP method. The reaction barriers for the *syn* and *anti* attack are 0.631 and 2.50 kcal mol^{-1} [B3LYP/6-311 + G(2d,p)], respectively.

[16] Intramolecular orbital interactions between the nonbonding orbitals on the carbonyl oxygen and the Group 14 metal–carbon antibonding orbitals are reported: K. Tani, S. Kato, T. Kanda, S. Inagaki, *Org. Lett.* **2001**, *3*, 655.

